www.czasopisma.pan.pl PAN POLSKA AKADEMIA NAUK www.journals.pan.pl

Arch. Metall. Mater., Vol. 61 (2016), No 1, p. 115–122

DOI: 10.1515/amm-2016-0022

Z. ŚWIĄTEK*,#, A.P. VLASOV**, M.V. IVASHKO**, R.L. PETRYNA**, A.YU. BONCHYK***, B.S. SOKOLOVSKII****

BARRIER STRUCTURES ON THE BASIS OF GRADED-BAND-GAP CdHgTe OBTAINED BY EVAPORATION-CONDENSATION-DIFFUSION METHOD

The paper presents the methods of obtaining photovoltaic structures based on $Cd_XHg_{1-X}Te$ graded-band-gap epitaxial layers. Barriers in these structures were formed by solid phase doping of the material with low-diffusing impurities (As). High-temperature diffusion of acceptor impurity (As) in intrinsically defective material of n-type conductivity as well as ion introducing the donor impurity (B) in uniformly doped during the epitaxy process material of *p*-type of conductivity have been used. The possibility of creating multi-element graded-band-gap photovoltaic structures suitable for broad band detection of infrared radiation as a result of epitaxial growth by evaporation-condensation-diffusion method has been demonstrated.

1. Introduction

Narrow-gap semiconductor solid solutions of cadmium and mercury telluride are the most suitable material for manufacturing highly efficient infrared detectors [1]. Mass production of $Cd_XHg_{1-X}Te$ is associated with considerable technological difficulties that have stimulated extensive study of its physical properties: for now, only Si and GaAs are investigated better than $Cd_XHg_{1-X}Te$. Global investment in the industry engaged in the development and application of devices based on $Cd_XHg_{1-X}Te$ amounts to billions of dollars. Intensification of research in leading scientific institutions in this field and growth of number of research centers that study the properties of both the material alone and devices on this material have both occurred recently. Currently, material for mass production of large multicolor matrix infrared photodetectors based on $Cd_XHg_{1-X}Te$ is obtained by low temperature epitaxy techniques, namely the molecular beam epitaxy (MBE) and metal organic vapour phase epitaxy compounds (MOVPE). These techniques provide reproducible means of obtaining a homogeneous material of large area and high quality. However, implementation and maintenance of such systems requires considerable resources and creation of functional structures requires complex application of high technological methods such as ion implantation, selective ion etching, etc. Therefore, for studying the material's properties and working out the technological operations $Cd_XHg_{1-X}Te$ layers obtained by different methods are used, particularly vapor phase epitaxy under isothermal conditions (ISOVPE). The latter is an equilibrium method of $Cd_XHg_{1-X}Te$ and does not require sophisticated equipment for carrying out the deposition process.The method is based on the direct transfer of HgTe onto the CdTe substrate. This scheme was proposed by the French researchers [2] and has been successfully used in many laboratories [3, 4]. The ISOVPE has several advantages [5, 6]: simplicity, perfect surface and relatively high electrophysical properties of the deposited layers. The main disadvantage of this method of epitaxy is assumed [7] to be the fact that the layers represent the structures of graded composition, that is have significant grading along the thickness of an epitaxial layer.

However, the applicability of the vapor epitaxy method is justified by its high efficiency, accessibility for the practical implementation of manufacturing graded-band-gap photosensitive structures in a single technological cycle. By purposeful choice of the profile one can control a wide range of parameters of the diffusion processes in the graded-band-gap material. The modern trends in $Cd_XHg_{1-X}Te$ device structures development in IR photo-electronics include the application of 3D band-gap engineering to the fabrication of uncooled photon detectors for wide spectral range on their basis. In such detectors, the multilayer structures operating in the non-equilibrium modes are used, with their operation relying on the magneto-concentration effect [8], negative luminescence [9], Dember effect [10, 11].

In this paper, we shall consider the methods of obtaining photovoltaic structures based on graded -gap epitaxial layers of $Cd_XHg_{1-X}Te$. The barriers in these structures were formed by solid-phase doping of the material with slowly diffusing acceptor impurity (As) with the aim of formation of both *p*- on *n*- , and *n*- on *p*- junctions. In the first case we used a high-temperature diffusion of the impurity into a material of *n*-type conductivity with intrinsic defects, in the second case – ion-based introduction of the donor impurities (B) into a material of *p*-type conductivity homogeneously doped in the process of epitaxy.

* INSTITUTE OF METALLURGY AND MATERIALS SCIENCE, POLISH ACADEMY OF SCIENCES, 25 REYMONTA STR., 30-059 KRAKOW, POLAND

** LVIV STATE UNIVERSITY OF PHYSICAL CULTURE, 11 KOSTIUSHKA STR., 79001, LVIV, UKRAINE

*** INSTITUTE FOR APPLIED PROBLEMS OF MECHANICS AND MATHEMATICS OF NASU, 3B NAUKOVA STR., 79601, LVIV, UKRAINE

**** IVAN FRANKO NATIONAL UNIVERSITY OF LVIV, 50 DRAGOMANOV STR., 79005 LVIV, UKRAINE

Corresponding author: z.swiatek@imim.pl

2. Experimental technique

For growth and subsequent thermal annealing of $Cd_XHg_{1-X}Te$ epitaxial graded-band-gap structures we used a modified technique of ISOVPE –evaporation-condensation-diffusion (ECD) [12]. This two-temperature and two-stage technique of carrying out the process in the closed system [13-15] is based on the precise control of temperature of the hot zone, T_p, and the vapor mercury pressure, P_{Hg}, in the zone of location of epitaxial structures $Cd_XHg_{1-X}Te$ (Fig. 1).

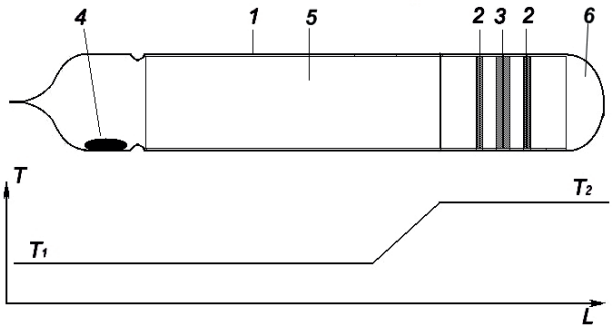

Fig. 1. Schematic of experimental set-up for growth: 1 – low-temperature zone of quartz ampoule; 2 – CdTe substrates; 3 – HgTe source; 4 – Hg drop; 5 –quartz accessories; 6 – high temperature zone of quartz ampoule

Usage of the two-temperature scheme allows one to conduct postgrowth annealing of samples without reloading. The use of annealing is a necessary condition for obtaining material with the required properties, which can be controlled by means of changing the intrinsically defect structure of the epitaxial layers. The undoped layers after long isothermal annealing (T = 300°C) at 77 K had n-type conductivity due to uncontrolled impurities (such as S.1 in Table 1). The experimental profile of the composition of this layer is shown in Fig. 2.

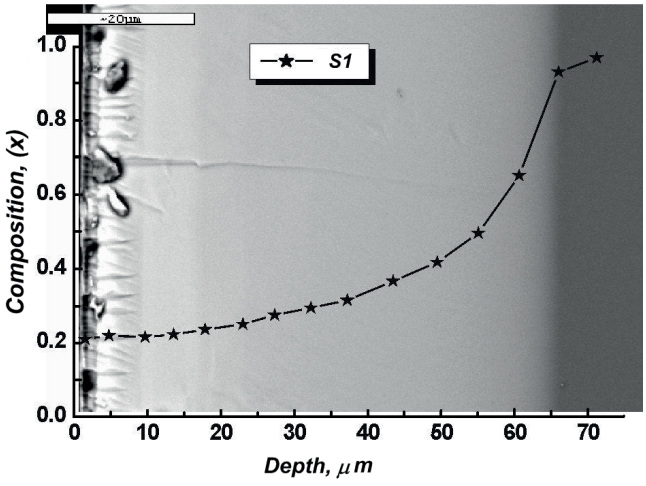

Fig. 2. SEM microphotography of cross cleavage and profile of composition distribution in sample S.1 of intrinsically defective epitaxial layer of ECD $Cd_XHg_{1-X}Te$

ECD epitaxy was used in order to obtain an impurity material of p-type conductivity. In process of ECD epitaxy the solid state doping of $Cd_XHg_{1-X}Te$ graded-band-gap layers from substrate is accomplished. The process of epitaxy from vapor phase is superimposed with solid state diffusion of impurity previously introduced into the substrate of undoped CdTe.

As solid sources of controlled impurity we used:

I. Homogeneously doped single crystals of CdTe grown by the Bridgman method with impurity introduced during the synthesis process with concentration N_{As}~ 10^{16}÷10^{17} cm $^{-3}$.
II. Intrinsically defective single crystals of CdTe, that had epitaxial heavily doped with As (N_{As}~ 10^{17} ÷ 10^{20} cm^{-3}) buffer films of $Cd_YHg_{1-Y}Te$ deposited on their surface.
III. Intrinsically defective single crystals of CdTe that had a controlled amount of As introduced on their surface by ion implantation.

Surface diffusant source surface of type II was made by high frequency (f = 13,56 MHz) sputtering in glow mercury discharge As doped wide-band-gap (Y > X) buffer epitaxial films of $Cd_YHg_{1-Y}Te$ (here and below Y denotes the composition of solid solution film with a diffusant, whereas X denotes the composition on the surface of graded-band-gap layers and uniform $Cd_XHg_{1-X}Te$ single crystals). In order to introduce As with concentrations greater than 1 at.% we used sputtering of the pure element together with the material of the target. For obtaining concentrations less than 0.01 at.% the impurity was introduced during synthesis of the target using As load. The content of impurities in the film was controlled by the surface from which sputtering took place. When using the impurities of type III As impurity was implanted with ions having the energies E = 100 keV. Ion implantation was carried out on an Ion-beam Installation MPB-202 produced by Balzers. The maximum pressure in the working chamber was 3.6 10^{-5} Pa. Calculation of the introduced dose was performed by an integrator with an accuracy of 0.02%. Heterogeneity of doping dose on the surface of samples did not exceed 1%, reproducibility was 98%.

The study of qualitative changes of composition of the main components of solid solution at their inter-diffusion and quantitative distribution of As along the thickness of $Cd_XHg_{1-X}Te$ structures was carried out on a Cameca IMS-6F by standard method of mass spectroscopy of secondary ions (SIMS). Types of diffusant sources used and typical resulting SIMS profiles of impurity distribution along the thickness of grown $Cd_XHg_{1-X}Te$ layers are presented in Fig. 3. Exponential decrease of its concentration in direction to the surface and the presence of diffusion barrier in the region of metallurgical boundary surface-epitaxial layer were observed. Electrophysical parameters of the obtained typical epitaxial structures, in particular Hall mobility μH and Hall coefficient R_H.measured by the van der Pauw method are presented in Table 1. Comparison of SIMS analysis and the concentration of charge carriers in the layers demonstrates electrical activity of the introduced impurity that is close to 100% (Table 1). A possibility of a controlled introduction of impurity exists in each case of such doping.

High-temperature solid phase doping of near-surface regions of graded-band-gap ECD epitaxial layers using the sources of II and III types was performed in order to create barrier structures in those layers. Regimes of heat treatment

TABLE 1

Electrophysical investigations of ECD $Cd_XHg_{1-X}Te$ epitaxial layers doped with As [14, 20]

Number of sample	Source of diffusant	X	d, μm	μ_H, cm²/V·s		R_H, cm³/C		$\lvert N_A–N_D\rvert$, cm⁻³ 77 K	n_{As}, (SIMS) cm⁻³
				273 K	77 K	273 K	77 K		
S.1	Undoped	0.23	64	7740	20050	–610	–1480	$4.2\cdot10^{15}$	-
S.2	Substrate	0.23	53	455	234	–146	+66	$9.6\cdot10^{16}$	$1\cdot10^{17}$
S.3	Substrate	0.20	66	6750	232	–650	+98	$6.4\cdot10^{16}$	$8\cdot10^{16}$
S.4	Substrate	0.21	57	3741	150	–293	+464	$1.35\cdot10^{16}$	$2\cdot10^{16}$
S.5	Buffer film	-	62	150	43	–91	+56	$1.12\cdot10^{17}$	$2\cdot10^{17}$
S.6	Ion Impl. surface	0.17	90	12400	32450	–80	–198	$3.17\cdot10^{16}$	$4\cdot10^{16}$
S.7	Ion Impl. surface	0.22	65	10340	5210	–110	+180	$1.3\cdot10^{16}$	$1.5\cdot10^{16}$

were selected to be close to the thermodynamic equilibrium in a closed system in which diffusion and inter-diffusion of the main component impurities and main components dominate, and the process of mass transfer through the vapor phase is retarded. The prepared heterostructures together with single crystal HgTe source located at some distance were rigidly mounted in the hot zone of quartz ampoule (Fig. 1). To ensure the required vapor pressure Hg that was subsequently regulated by the temperature of the cold zone, a certain mass of pure mercury in liquid phase was added into ampoules. Ampoules were pumped using oil-free pumps to the residual pressure ~ 10^{-4} Pa. Afterwards they were loaded into a two-zone resistive furnace, where a diffusion annealing of the impurity and its activation at $T = (500 \div 600)$°C have occurred.

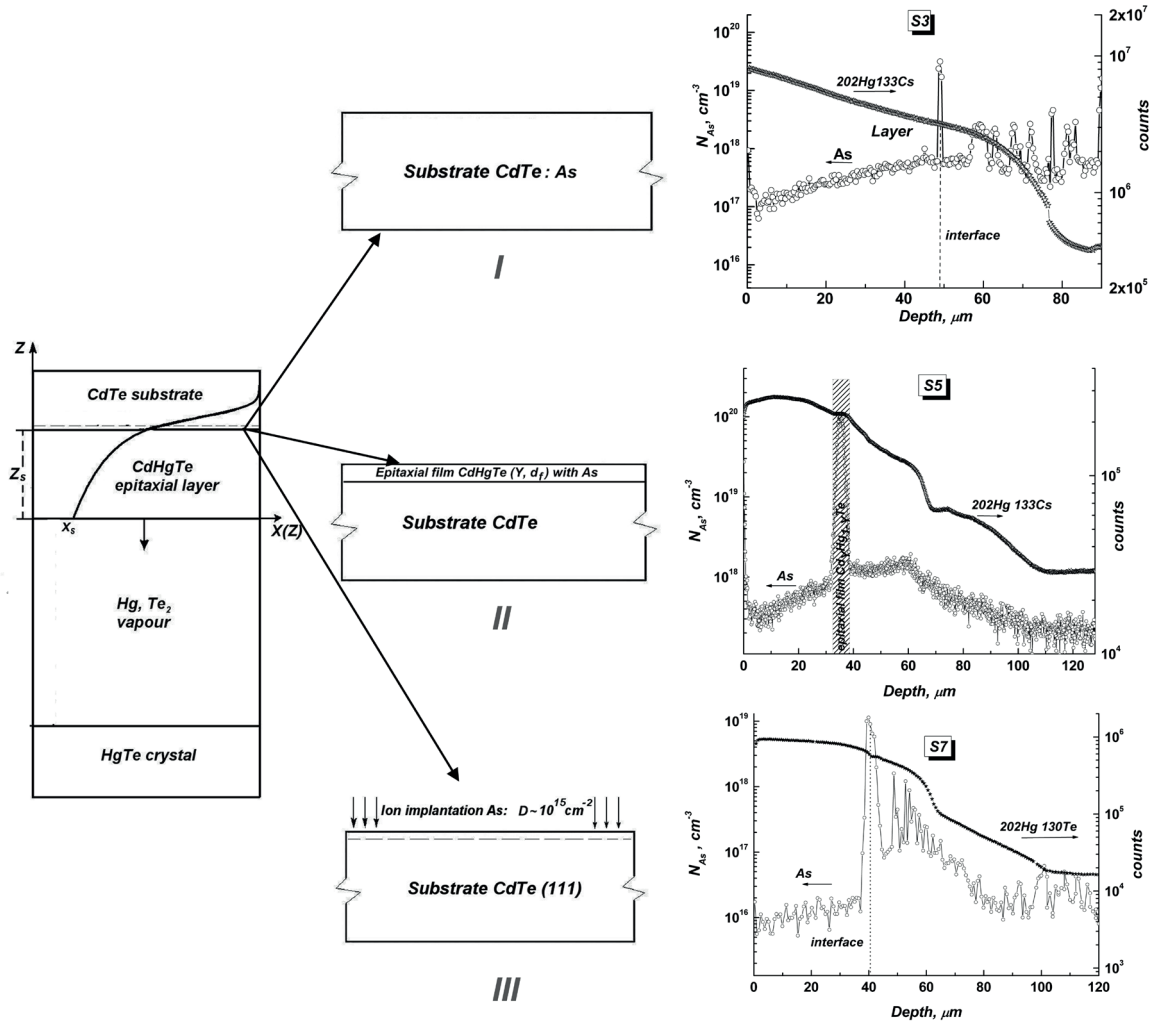

Fig. 3. Technique of solid phase doping with acceptor impurity of EDC layers during the process of epitaxial growth. Schemes of cross section of initial heterostructures and SIMS distribution of impurity and signal of the main component of CdHgTe solid solution of EDC epitaxial layers

Upon completion of the diffusion process the furnace's temperature was decreased to 300°C without overloading the ampoules and a low-temperature annealing of samples for 72 hours in an atmosphere saturated with mercury vapor was performed, in order to reduce the concentration of mercury vacancies formed during high temperature heat treatment to the level lower than concentrations of uncontrolled impurities, and to return undoped base of the layer to the initial state by the defect structure. Cooling of ampoules after annealing was carried out directly in the oven after switching them off. The developed technique of multistage thermal annealing of epitaxial layers and structures based on Cd_XHg_{1-X} in vapor of solid solution components for the temperatures in range T = 150 - 600°C [18, 19] ensured the preservation of the crystal structure of near-surface regions of experimental samples [20] and allowed us to use them to create photovoltaic structures [21].

Composition (X) of the ECD epitaxial layers of Cd_XHg_{1-X} was controlled by optical absorption spectra and long-wavelength photoconductivity cut-off. The type of conductivity, carrier concentration (N_a-N_d) and mobility (μ_H) at 77 K were determined by a standard method of measuring amplitude in the range of magnetic fields 0÷1.8 T. (Table 1). Electrical activity of impurities was measured by determining the depth of location of p-n junction (d_j) by means of direct observation of the latter in the electron microscope in the EBIC regime on the cleavage of the diode structure created by mesa-technology, as well as by measurements of thermo e.m.f. at T = 77 K on test mesa-structures.

3. Experimental results

Formation of photovoltaic barrier structures of p- on n-type in $Cd_XHg_{1-X}Te$ graded-band-gap epitaxial layers was carried out by means of solid phase doping of the material with slowly diffusing acceptor impurity (As) during the processs of heat treatment (T = 500÷600°C) or ECD epitaxial growth.

3.1. Diffusion barrier structures (p- on n- type) obtained by high temperature annealing

3.1.1 Using doped epitaxial films of $Cd_xHg_{1-x}Te$ as diffusant source

In order to form a barrier structure of p-on n- type, we have used solid phase source of As on the surface of ECD $Cd_XHg_{1-X}Te$ epitaxial layers that was created by the method of epitaxial deposition of $Cd_yHg_{1-y}Te$: As film in the high frequency mercury plasma with localization of discharge in a quasi-closed volume [8] at deposition temperature 235°C. We used alloy targets based on CdTe-Te for RF sputtering. Content of the targets ensured formation of the resulting epitaxial $Cd_yHg_{1-y}Te$ with the necessary composition y ≈ X. One can note the correspondence of these values along the 202Hg133Cs signal line in the resulting structure (Fig. 4). As impurity was introduced into the target during its fabrication. We used the targets with As concentration close to $4\cdot10^{17}$cm^{-3} for deposition of doped films in the studied heterostructures; the films with high concentration of As were deposited onto the target doped with As up to 10^{20} cm^{-3}. The target was sputtered onto surfaces of the corresponding substrates freshly etched in bromine-methanol etchant. S8, S9, S10 heterostructures were obtained as a result of the above procedures. Their cross sections are shown in Fig.4, a. Electrophysical properties of the ECD layers of $Cd_XHg_{1-X}Te$, determined before deposition of As doped $Cd_yHg_{1-y}Te$:As epitaxial film or before ion implantation of the impurity, and characteristics of diffusant sources are presented in Table 2.

Profile of As distribution and 202Hg133Cs signal along the depth of diffusion structures after thermal treatment [T= 500°C; P_{Hg} = 2,9×10^5 Pa; treatment in diffusion regime for one hour] obtained by secondary mass spectrometry is shown in Fig. 4b. The dash-dot line shows position of the initial metallurgical boundary between the As doped epitaxial film and ECD epitaxial layer, as well as the concentration of electrons in the base material (background). This level is determined by galvanomagnetic measurements on the test sample of resulting structure S9, that had its surface layer chemically etched away. The etched layer was thicker than the maximum depth of penetration of impurities after the diffusion process. The obtained values correlate well with the initial concentration of carriers in the initial ECD epitaxial layer.

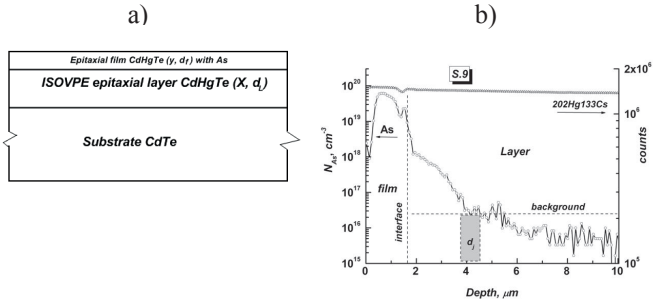

Fig. 4. Scheme of cross section of initial heterostructures S8, S9, S10 (a); SIMS distribution of As and signal of the main component of $Cd_XHg_{1-X}Te$ solid solution (Hg concentration) in near-surface regions for heteroepitaxial structure of sample S9 (b)

On the basis of these structures photosensitive elements with unprotected surface have been fabricated. The wavelength

TABLE 2

Electrophysical properties of substrates measured before introducing impurity and characteristics of diffusant sources

Sample	X	d_L, μm	N_D-N_A, cm^{-3}	μ_H, cm^2/V.s	Diffusant source		
					y	d_f, μm	n_{As}, cm^{-3}
S8	0.22	59	$1.1\cdot10^{16}$	$3.2\cdot10^4$	0.22	4	≈$4\cdot10^{17}$
S9	0.25	58	$2.5\cdot10^{16}$	$2.7\cdot10^4$	0.22	1.7	≈10^{20}
S10	0.24	60	$2.8\cdot10^{16}$	$2.6\cdot10^4$	0.22	7.4	≈10^{20}
S11	0.22	62	$5.1\cdot10^{15}$	$4.2\cdot10^4$	0.3/0.22	2/1	≈10^{19}/≈$5\cdot10^{20}$

at half of the maximum photosensitivity determined from the spectral distribution of photo-response of diodes in sample S9 (Fig. 5) is 5.5 μm. Weak photo-response in the long-wavelength region of these structures is most probably related to the fact that the *p*-region of *p*+ - *n* junction is formed by $Cd_XHg_{1-X}Te$ with a gap narrower than in *n*-type base. Therefore, the carriers generated in the narrow-gap part will not be separated because of the potential barrier in the conduction band of $Cd_XHg_{1-X}Te$.

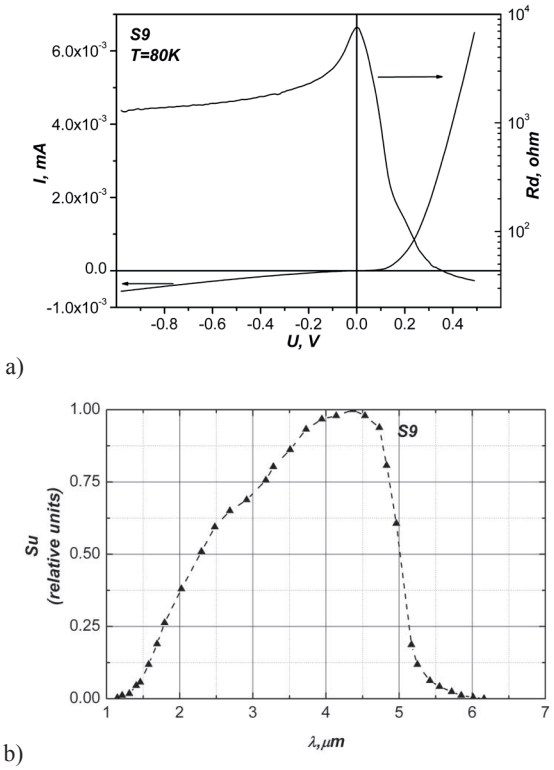

Fig. 5 Volt-ampere characteristics (VAC) of p^+-*n* photodiodes fabricated on the basis of diffusion structures of sample S (a) and spectral distribution of photo-signal in the photodiode fabricated on the basis of this sample (b)

Usage of the low-temperature epitaxy in the form of RF sputtering in Hg glow discharge on the EDC layers of $Cd_XHg_{1-X}Te$ and subsequent diffusion annealing enables a formation of complex multilayer heterostructures (Fig.6a), in which impurity concentration and composition of the deposited film of $Cd_yHg_{1-y}Te$ vary in wide ranges. The scheme of cross section of the initial structure is shown in Fig.6a and SIMS distribution of As and 202Hg133Cs signal in the near-surface region of three-layer diffusion heterostructure S11 after thermal annealing is presented in Fig. 6b. Modulation of doping impurity concentration and step-like character of changes in the solid solution composition ($y_2>y_1>X$) are realized in the structure. The material of such type can be used for creation of non-cooled IR detectors.

a) b)

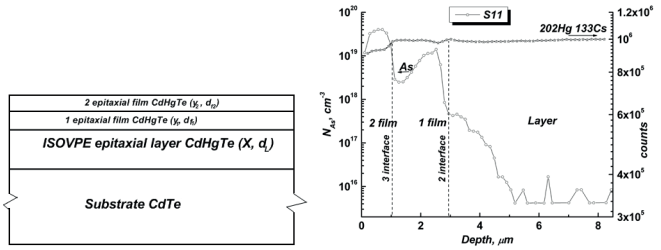

Fig.6. Scheme of cross section of initial heterostructure S11 (a); SIMS distribution of As and signal of the main component of CdXHg1-XTe solid solution (Hg concentration) in near-surface regions for hetero-epitaxial structure of sample S11 (b)

3.1.2 The use of ion implantation of impurity (S12)

Classical example of forming barrier structure of *p*-on *n* type is heterostructure S12 (Fig.7) obtained by ion implantation of As in EDC epitaxial layer of $Cd_XHg_{1-X}Te$. Properties of this layer determined before implantation and regimes of the latter are indicated in Table 2.

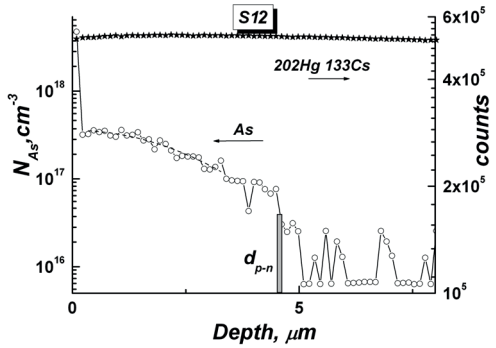

Fig. 7. SIMS distribution of As and signal of the main component of $Cd_XHg_{1-X}Te$ solid solution (Hg concentration) in near-surface regions for heteroepitaxial structure of sample S12

Diffusion structure S12 was obtained after the diffusion process performed at the temperature T=500°C, P_{Hg}= 2.9×10⁵ Pa for four hours. SIMS analysis of the near-surface region of the obtained heterostructure has shown the classical profile of impurity distribution in active region of the structure (Fig.7). The location of *p*-*n* junction for photodiodes made by mesa technology with unprotected surface was determined by the EBIC method; it depends to large extent on intrinsically defective structure of the basic epitaxial material. Fig. 8a shows VAC and dependence of the normalized differential resistance on voltage at T~80K and Fig.8b demonstrates spectral distribution of photoresponse normalized by the power of black body radiation with the temperature equal to

TABLE 3

Electrophysical properties of substrates measured before introducing impurity and characteristics of diffusant sources

Sample	X	d_L, μm	N_D-N_A, cm^{-3}	μ_H, cm^2/V.s	E, кеV	D, cm^{-2}
S12(As)	0.26	63	$1.1\cdot10^{15}$	$2.7\cdot10^4$	80	$5\cdot10^{15}$
S3 (B)	0.20	66	$7.8\cdot10^{16}(p)$	232	40	$8\cdot10^{14}$

1440K (globar) (without taking into account transmission spectrum of optical system of YKS-21). The wavelength at half of maximum of signal for this photodiode is λ_{co}=4.7 μm.

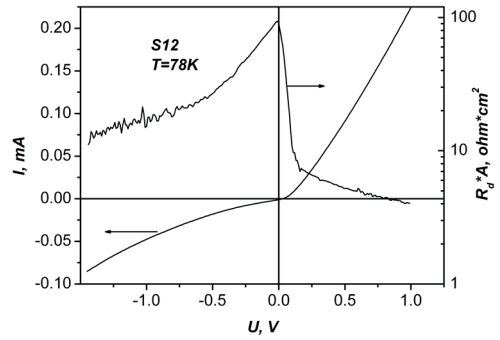

a)

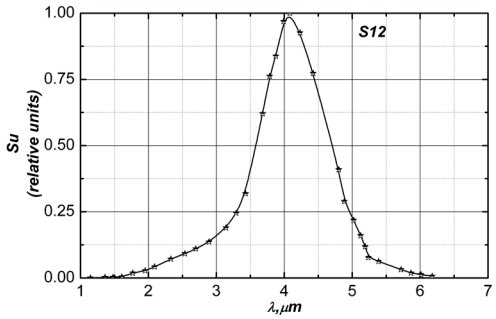

b)

Fig. 8. VAC and dependence of differential resistance normalized by square of voltage for the photodiode obtained in diffusion structure of sample S12 (a). Spectral distribution of photo-signal of photodiode obtained from sample S12 (b)

3.2. Diffusion barrier structures (*n*- on *p*- type) based on ion-implanted layers

In order to reduce the influence of intrinsic defects of $Cd_XHg_{1-X}Te$ base material on photoelectric properties of barrier structures, the latter were manufactured using the active and base parts of ECD graded-band-gap epitaxial layers doped with donor (B) and acceptor (As) impurities, respectively. For fabrication of such structures we have used $Cd_XHg_{1-X}Te$ homogeneously doped with As during epitaxial growth (S3, Table 1), into which B ions were implanted (*E=100keV*; $D = 5 \cdot 10^{15} cm^{-2}$). After completion of implantation the heterostructure was annealed at $T = 200°C$ for 24 hours in order to heal the surface radiation damages of crystal lattice, diffuse bor onto the necessary depth, and activate it. Fig. 9 presents the SIMS profileof distribution of As, B and the main component in the near-surface region of the resulting heterostructure, as well as the results of integrated galvanomagnetic measurements. The depth of *p-n* junction in this heterostructure determined by measurement of currents induced by an electron beam (EBIC) is caused in the limit of error by the controlled introduction of acceptor and donor impurities into epitaxial $Cd_XHg_{1-X}Te$.

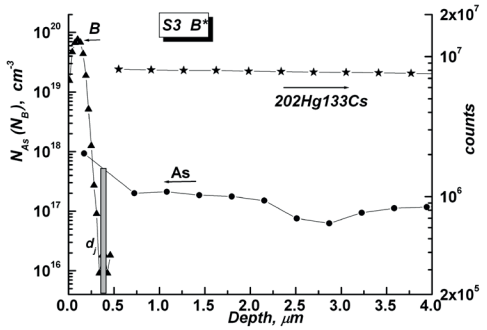

Fig. 9. SIMS distribution of As and signal of the main component of $CdXHg_{1-X}Te$ solid solution (Hg concentration) in near-surface regions for epitaxial structure of sample S3 B*

Typical appearance of the fragment of one-dimensional array of photodiodes fabricated by mesa-technology with unprotected surface is seen on the microphotography in Fig.10a. The spectral characteristic of one of the elements with an area of 250×250 μm^2 and formed contact groups is shown in Fig. 10b.

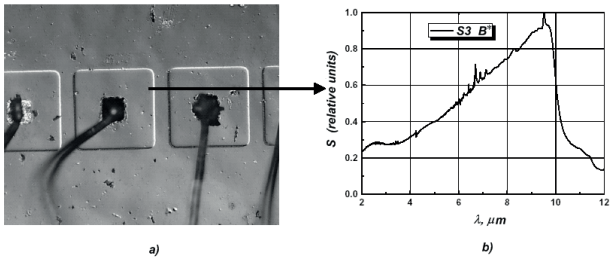

Fig. 10. Fragment of photodiode one-dimensional array of photodiodes a);spectral characteristic of a photodiode from that array b)

3.3. Three-dimensional barrier structures (p- doped inclusion in n-base material) obtained by local diffusion during ECD epitaxy

Modern epitaxial techniques made it possible to grow complex 3D-heterostructure, that enable creation of highly efficient optoelectronic devices through precise control of the band structure and doping level [22]. Such heterostructures are obtained by means of band engineering using a combination of experimental techniques, in particular the repeated and selective epitaxial growth. Fabrication of this type of photovoltaic structures based on $Cd_XHg_{1-X}Te$ for detecting long-wavelength IR at close to room temperatures is presented in [23].

We have demonstrated the possibility of creating vertical graded-band-gap photovoltaic structures using local doping during high-temperature ECD epitaxy, schematic view of which is shown in Fig. 11a. In order to achieve this, implanted with As (E = 100keV, $D = 1 \cdot 10^{15}$ cm $^{-2}$) substrates of undoped CdTe (111) were used as a source of impurity.

Island structures with dimensions of 80 × 80μm^2 and a step of 350 mm were formed by photolithography. Photoresist served as a mask during chemical etching of unprotected surface of CdTe substrate in a bromine-containing etchant. Etching was carried out to a depth of about 1 μm, which exceeds the distance of maximum penetration of As ions during implantation with appropriate regimes for CdTe that is known from SIMS analysis. Thus we made a local source of impurity on the substrate for the epitaxy process and provided visualization of the location of the resulting structures after the completion of implantation. Photography of the island structure on the working surface of CdTe substrate is shown in Fig. 11 b. The $Cd_{0.18}Hg_{0.82}Te$ graded-band-gap layer was grown after completing preparatory procedures on this substrate with standard regimes of ECD epitaxy. Photograph of the surface of thus obtained epitaxial structures in monolithic form is shown in Fig. 11 c. Estimation of As penetration during epitaxy at T = 600°C shows that the impurity diffuses at distances up to 100 μm, which slightly exceed the thickness of the grown MCT epitaxial layer. Given that these structures are naturally graded-band-gap ones (Eg changes from 1.6 eV in CdTe substrate to 0.1 eV on the surface layer $Cd_{0.2}Hg_{0.8}Te$), it is possible to create several color structures photosensitive in IR range. Their schematic diagram is shown in Fig. 12. The steps of different height include the photosensitive elements formed by chemical etching of surfaces with structures unprotected with photoresist, performed several times. Multiplicity and etching depth specify number and range of IR detection. The range of detection is determined by the band gap of near-surface layer of the sensitive element, which is dependent on the thickness of graded-band-gap and is determined by the etching depth. Such devices are an example of 3-D photovoltaic detectors of broadband IR and may be used for fabrication of multicolored monolithic IR detectors in the future.

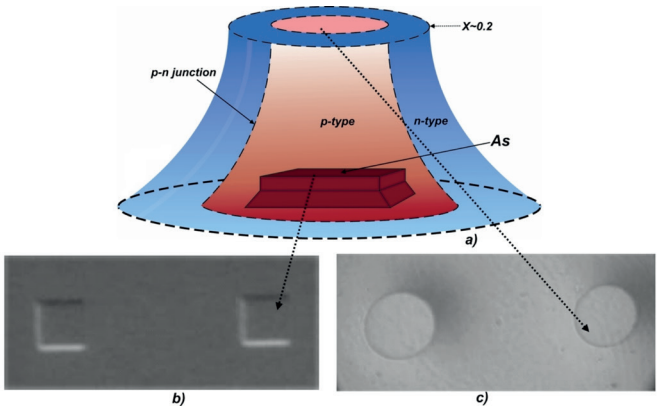

Fig 11. Schematic view of an element of 3-D diffusion structure a); island structures of 80x80 μm^2 dimensions with As implanted surface formed on undoped CdTe (111) substrate b); relief of epitaxial structures obtained by ECD epitaxy of $Cd_{0.18}Hg_{0.82}Te$ on island substrate of CdTe c)

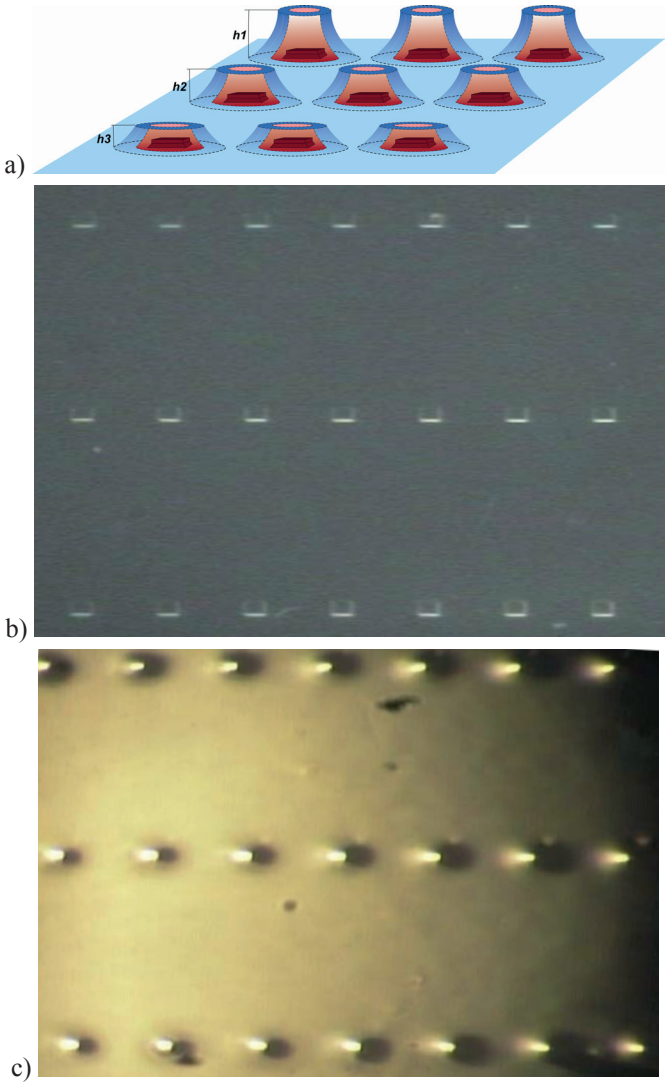

Fig 12. Schematic view of a fragment of 3-color monolithic matrix a); island structures of 80x80 μm^2 dimensions with As implanted surface formed on undoped CdTe substrate b)

4. Conclusions

In this work, it has been developed a method of doping of $Cd_XHg_{1-X}Te$ with As impurity which allows one to effectively dope the material in the process of epitaxial growth. Diffusion techniques for creating impurity photovoltaic structures based on $Cd_XHg_{1-X}Te$ grown by ECD epitaxy with solid-state diffusant sources are presented. RF sputtering in mercury glow discharge or impurity implantation and annealing in vapor of solid solution components in a wide temperature range (150-600°C) were used for the controlled introduction, diffusion and activation of impurities. The study is mainly focused on the construction of a material of p-type conductivity doped with As. This slowly diffusing impurity and fast processes

of inter-diffusion of main components of $Cd_XHg_{1-X}Te$ make it possible to create graded-band-gap barrier structure suitable for detection of infrared radiation. The possibility to create multi-component photovoltaic graded-band-gap structures suitable for broadband detection of IR during the ECD epitaxial growth process is experimentally established.

REFERENCES

[1] A. Rogalski, Defence Science Journal **51**(1),5-34 (2001).
[2] G. Cohen-Solal, Y. Marfaing, F. Bailly, Phys.Appl. Rev.**6** , 11-17 (1966).
[3] J. Piotrowski, A. Piotrowski, Opto-Electr. Rev. **14**(1), 37–45 (2006).
[4] U. Gilabert, E. Heredia, A.B. Trigubo, Thin Solid Films **317**, 1-6 (2006).
[5] B. Koo, J. Wang, Y. Ishikawa, C.G. Lee, M. Isshiki, Jpn. J. Appl. Phys. 37, 4082-4085 (1998).
[6] J.-G. Lo, H. Lan, J.-Y. Chen, L.S. Lu, Jpn. J. Appl. Phys. **30**(8), 1770-1774 (1991).
[7] V.S. Varavin, Yu.G. Sidorov, V.G. Remesnyk, S.I. Chikichev, I.E. Nis, Fizika i technika poluprovodnikov **28**(4), 577-583 (1994) (In Russian).
[8] V.G. Savitskii, B.S. Sokolovskii, M.I. Stodilka, V.I. Furman, Ukrainskii fizicheskii zurnal **23**(5), 792-797 (1978) (In Russian).
[9] B.S. Sokolovskii, Semiconductors **30**(6), 361-1368 (1996).
[10] B.S. Sokolovskii, V.I. Ivanov-Omskii, G.A. Il'chuk, Semiconductors **39**(12), 1361-1368 (2005).
[11] B.S. Sokolovskii, V.K. Pysarevskii, O.V. Nemolovskii, Z. Swiatek, Thin Solid Films 431-432, 457-460 (2003).
[12] Method of growth of epitaxial layers of solid solutions on the basis of chalcogenides of mercury. V.G. Savitskii, L.I. Aleksenko, Patent of USSR, No. 668505, 12.04.1977 (In Russian).
[13] V.G. Savitsky, O.P. Storchun, Thin Solid Films **317**, 105-107 (1998).
[14] A. Vlasov, V. Pysarevsky, O. Storchun, A. Shevchenko, A. Bonchyk, H. Pokhmurska, A. Barcz, Z. Swiatek, Thin Solid Films **403-404**, 144-147 (2002).
[15] A.P. Vlasov, A.Yu. Bonchyk, I.M. Fodchuk, R.A. Zaplitnyy, A. Barcz, Z. Swiatek, Semiconductor Physics, Quantum Electronics & Optoelectronics **9**(1), 36-42 (2006).
[16] Method of obtaining epitaxial layers of binary semiconductor alloys. L.I. Alekseenko, N.N. Berchenko, V.E. Krevs, I.E. Maronchuk, Yu.G. Pukhov, V.G.Savitskii, A.R. Filatova, Patent of USSR , No.668504, 23.07.1975 (in Russian).
[17] Technique of cover deposition. V.G. Savitskii, L.G. Mansurov, M.V. Miliyanchuk, B.A. Simkiv, Patent of USSR, No. 1480362, 04.08.1987 (in Russian).
[18] A. Vlasov, V. Bogoboyashchyy, O. Bonchyk, A. Barcz, Cryst. Res. Technol. **39**(1), 11-22 (2004).
[19] A. P. Vlasov, B.S. Sokolovskii, L.S. Monastyrskii, O.Yu. Bonchyk, A. Barcz, Thin Solid Films **459**(1-2), 28-31 (2004).
[20] A.P. Vlasov, A.Yu. Bonchyk, I.M. Fodchuk, R.A. Zaplitnyy, A. Barcz, Z. Swiatek, Semiconductor Physics, Quantum Electronics & Optoelectronics **9**(1), 36-42 (2006).
[21] A.P. Vlasov, V.K. Pysarevsky, A.V. Shevchenko, A.Yu. Bonchyk, A. Barch, Proc. SPIE (5126), 391-397 (2003).
[22] J. Piotrowski, M. Grudzien, Z. Nowak, Z. Orman, J. Pawluchyk, M. Romanis, W. Gawron, Proc. SPIE **4130**, 175-184 (2000).
[23] W. Gawron, A. Rogalski, Infrared Physics & Technology 43, 157-163 (2002).

Received: 20 February 2015.